ACS APPLIED MATERIALS & INTERFACES

Research Article

www.acsami.org

Double-Layer Ionomer Membrane for Improving Fuel Cell Performance

Takashi Mochizuki,[†] Makoto Uchida,[‡] Hiroyuki Uchida,[‡,§] Masahiro Watanabe,*[,‡] and Kenji Miyatake*[,‡,§]

[†]Interdisciplinary Graduate School of Medicine and Engineering, [‡]Fuel Cell Nanomaterials Center, and [§]Clean Energy Research Center, University of Yamanashi, 4 Takeda, Kofu, Yamanashi 400-8510, Japan

Supporting Information

ABSTRACT: A double-layer ionomer membrane, thin-layer Nafion (perfluorinated sulfonic acid polymer) on a sulfonated aromatic block copolymer (SPK-*bl*-1), was prepared for improving fuel cell performance. Each component of the double-layer membrane showed similar phase-separated morphologies to those of the original membranes. A fuel cell with the double-layer membrane exhibited lower ohmic resistance and higher cathode performance than those with the original SPK-*bl*-1 membrane despite their comparable water uptake and proton conductivity. Detailed electrochemical analyses of fuel cell data suggested that the thin Nafion interlayer contributed to improving the interfacial contact between the SPK-*bl*-1 membrane and the cathode catalyst layer and to mitigating excessive drying of the membrane. The results provide new insight on designing high-performance fuel cells with nonfluorinated ionomer membranes such as sulfonated aromatic polymers.

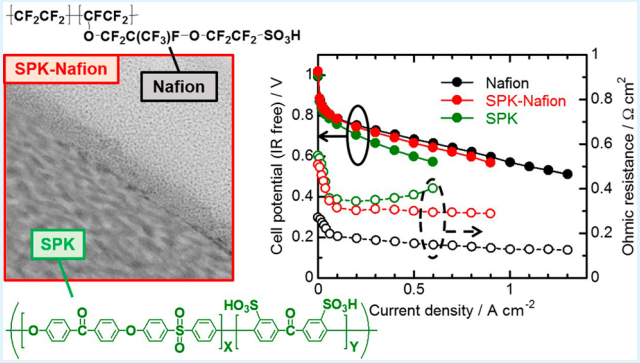

KEYWORDS: *fuel cells, proton exchange membranes, double-layer membranes, cathode*

INTRODUCTION

Polymer electrolyte fuel cells (PEFCs) have attracted much attention due to their applications as residential cogeneration systems and automotive power sources. Perfluorosulfonic acid (PFSA) ionomers such as Nafion (Du Pont) have been most used as the electrolyte membranes for PEFCs. However, several problems, such as high production cost, high gas permeability, and environmental incompatibility, are concerns for widespread commercialization of fuel cells.[1−3] To overcome these drawbacks, nonfluorinated aromatic hydrocarbon ionomer membranes have been extensively investigated as alternatives to PFSAs.[4−6] It has been reported that some aromatic ionomer membranes have shown comparable performance and durability compared to PFSA ionomer membranes in operating fuel cells.[7−9] However, their fuel cell performances often drop under low-humidity conditions. Furthermore, we observed that the cathode catalytic performance was worse with aromatic ionomer membranes than with PFSA ionomer membranes even though the same cathode catalyst layers (same Pt loading and PFSA binder) were used. It is well recognized that the interfacial contact between the ionomer membrane and the catalyst layer significantly affects on the cathode performance. Kim et al. reported that low water uptake interlayer improved compatibility with Nafion-bonded catalyst layers and accordingly enhanced performance and durability of a direct methanol fuel cell with aromatic ionomer membrane.[10] However, the effect of such interlayer on the cathode performance has not been investigated.

In this research, we focus on the interfacial structures between the ionomer membranes and the catalyst layers and their impact on the fuel cell cathode performance. Our approach includes preparation of a double-layer ionomer membrane composed of a thin Nafion layer on top of our block copolymer ionomer membrane. The double-layer membrane was characterized by SEM, TEM, water uptake, and proton conductivity and subjected to electrochemical investigations in fuel cells.

EXPERIMENTAL SECTION

Ionomer Membranes and Measurements. Nafion NRE 211 (ion exchange capacity (IEC) = 0.91 mequiv g^{-1}) was purchased from Du Pont. SPK-*bl*-1 (IEC = 2.34 mequiv g^{-1}) was synthesized in house.[8] The membrane thicknesses of NRE 211 and SPK-*bl*-1 were 25 and 24 μm, respectively. The molecular structures of these ionomer membranes are depicted in Figure 1. The double-layer ionomer membrane, SPK−Nafion, was prepared with spraying Nafion dispersion solution, which consisted of Nafion ionomer (IEC = 0.95−1.03 mequiv g^{-1}, D-521, Du Pont), pure water, and ethanol, onto an SPK-*bl*-1 ionomer membrane with a purse-swirl spray (PSS) apparatus (Nordson). The target value of the thickness of the Nafion

Received: May 26, 2014
Accepted: July 2, 2014
Published: July 2, 2014

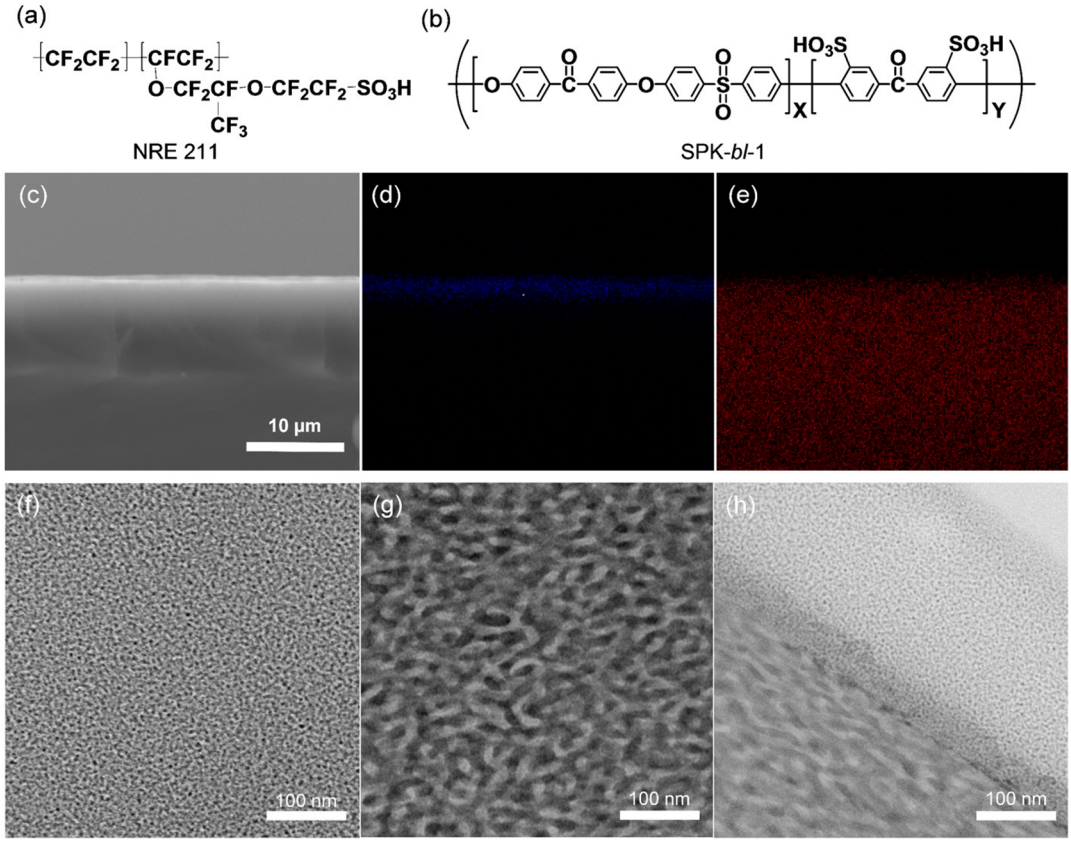

Figure 1. Molecular structures of the ionomer membranes: (a) NRE 211 (DuPont) and (b) SPK-*bl*-1 (synthesized in-house). (c) Cross-sectional SEM image and elemental mapping of (d) fluorine and (e) sulfur in the SPK–Nafion ionomer membrane. TEM images of (f) NRE 211, (g) SPK-*bl*-1, and (h) SPK–Nafion ionomer membranes. Samples were ion exchanged with lead (Pb^{2+}) ions prior to observation so as to stain the hydrophilic domains in black.

layer was 0.5 μm, which was the smallest value to ensure the uniform coating with the apparatus. The prepared SPK–Nafion membrane was dried at 60 °C for 6 h and hot pressed at 140 °C and 10 kgf cm^{-2} for 3 min. Scanning electron microscopy (SEM) was carried out for the SPK–Nafion membrane using a Hitachi S-3000N at an acceleration voltage of 20 kV. Energy-dispersive X-ray (EDX) analysis was also employed for elemental mapping of fluorine and sulfur. Transmission electron microscopy (TEM) was carried out for the three ionomer membranes (NRE 211, SPK-*bl*-1, and SPK–Nafion) in lead ion form using a Hitachi H-9500 at an acceleration voltage of 200 kV. Water uptake and in-plane proton conductivity of the membranes were measured with a solid electrolyte analyzer system (MSBAD-V-FC, Bel Japan Co.) at 80 °C with varying humidity conditions from 20% to 95% RH (relative humidity). Proton conducting resistance was measured using a four-probe conductivity cell attached with impedance spectroscopy (Solartron 1255B and 1287).

Preparation of Catalyst-Coated Membranes (CCMs). The catalyst paste was prepared by mixing the Pt/CB catalyst (TEC10E50E, Tanaka Kikinzoku Kogyo K. K.), Nafion binder (IEC = 0.95–1.03 mequiv g^{-1}, D-521, Du Pont), pure water, and ethanol by ball milling for 30 min. The mass ratio of Nafion binder to the carbon support (N/C) was adjusted to 0.70. The catalyst-coated membranes (CCMs) were prepared by spraying the catalyst paste on both sides of the three ionomer membranes (NRE 211, SPK-*bl*-1, and SPK–Nafion) by use of the PSS technique. The CCMs were dried at 60 °C for 6 h and hot pressed at 140 °C and 10 kgf cm^{-2} for 3 min. The geometric area and Pt-loading amount of the catalyst layer (CL) were 29.2 cm^2 and 0.50 ± 0.03 mg cm^{-2}, respectively. The CCMs were sandwiched between two gas diffusion layers (GDL, 25BCH, SGL Carbon Group Co., Ltd.) and mounted into a Japan Automobile Research Institute (JARI) standard cell, which has serpentine flow channels on both the anode and the cathode carbon separators. For the SPK–Nafion membrane, a thin Nafion layer was placed on the cathode side. The cells using NRE 211, SPK-*bl*-1, and SPK–Nafion are denoted as NRE211-cell, SPK-cell, and SPK–Nafion-cell, respectively.

Fuel Cell Operation. The electrochemically active surface area (ECSA) of the Pt catalyst at the cathode was estimated by cyclic voltammetry at 80 °C at 30%, 53%, 80%, and 100% RH using a potentiostat (PGST30 Autolab System, Eco-Chemie). Prior to the cyclic voltammogram measurements, hydrogen (100 mL min^{-1}) and nitrogen (150 mL min^{-1}) were supplied to the anode and cathode, respectively. Before the potential sweep, the cathode potential was maintained at 0.07 V for 3 s. Then, the nitrogen flow was stopped and the potential swept from 0.07 to 1.0 V at a sweep rate of 20 mV s^{-1}. ECSA values were calculated from the hydrogen adsorption charge in the negative-going potential scan, referred to ΔQ_H^0 = 0.21 mC cm^{-2}, adopted conventionally for clean polycrystalline platinum.[11] Linear sweep voltammetry (LSV) was measured to investigate the permeation of hydrogen gas flowing from the anode to the cathode through the ionomer membranes. LSV measurements were carried out at 80 °C. Prior to the measurements, hydrogen (100 mL min^{-1}) and nitrogen (150 mL min^{-1}) humidified at 30%, 53%, 80%, and 100% RH were supplied to the anode and cathode, respectively. The cathode potential was swept from 0.15 to 1.0 V at a sweep rate of 0.5 mV s^{-1}. To evaluate the cell performance, the polarization curves were measured at 80 °C. Pure hydrogen and air humidified at 30%, 53%, 80%, and 100% RH was supplied to the anode and cathode, respectively. Gas utilization at the anode and cathode was 70% and 40%, respectively. The high-frequency resistance (HFR) of the cell was measured with an AC milliohmmeter (model 3356 Tsuruga Electric Corp.) at 1.0 kHz.

RESULTS AND DISCUSSION

Characterization of Double-Layer Ionomer Membrane. The molecular structures of the ionomer membranes, Nafion NRE 211 and SPK-*bl*-1, are depicted in Figure 1a and 1b. A double-layer membrane, thin-layer Nafion on SPK-*bl*-1, was prepared by a spray-coating method. The cross-sectional scanning electron microscopic (SEM) images and elemental mapping of fluorine and sulfur of the double-layer membrane are shown in Figure 1c, 1d, and 1e. A very thin (ca. 0.55 μm) Nafion layer was observed on top of the 24 μm thick SPK-*bl*-1 membrane (Figure 1c). The Nafion layer was flat with no detectable pinholes throughout the field of view. In the EDX analyses, sulfur atoms were detected in both layers while fluorine atoms were detected only in the thin layer. The results indicate successful preparation of the double-layer ionomer membrane with distinct interfaces between the two components. In Figure 1f, 1g, and 1h are compared transmission electron microscopic (TEM) images of Nafion NRE 211, SPK-*bl*-1, and SPK–Nafion double-layer membranes in Pb^{2+} ion forms, respectively. Nafion NRE 211 exhibited the well-known phase-separated morphology with spherical hydrophilic domains (represented in black) of 3–6 nm in diameter distributed uniformly throughout the field of view (Figure 1f). SPK-*bl*-1 exhibited belt-like hydrophilic domains of ca. 5–15 nm in width surrounding large hydrophobic domains of ca. 10–20 nm in width (Figure 1g). The SPK–Nafion double-layer membrane exhibited two layers, each of whose morphology was very similar to that of the original component (Figure 1h). The minor difference in IEC values between NRE 211 (0.91 mequiv g^{-1}) and thin-layer Nafion (0.95–1.03 mequiv g^{-1}) was unlikely to lead to morphological differences. The interface was clear, with a very thin mixed interlayer (ca. 40–50 nm).

Figure 2 shows water uptake and proton conductivity of the three ionomer membranes (Nafion NRE 211, SPK-*bl*-1, and SPK–Nafion) measured at 80 °C as a function of relative humidity (RH). SPK–Nafion showed water uptake and proton conductivity very similar to those of the SPK-*bl*-1 membrane within acceptable error at all humidities. This result is reasonable, taking into account the fact that the volume content of the thin Nafion layer was low (2.3%) in the double-layer membrane. It also indicates that the interfacial contact between Nafion and SPK-*bl*-1 was good, as expected from the SEM and TEM images mentioned above.

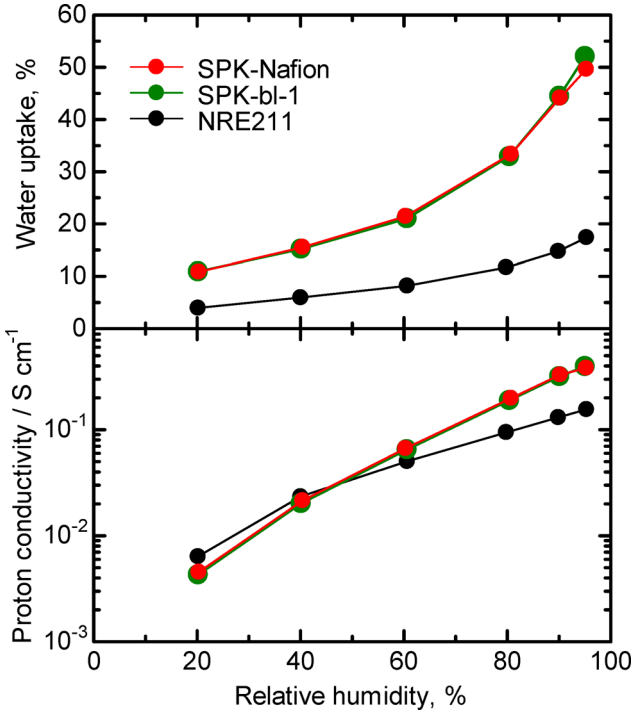

Figure 2. Water uptake and proton conductivity of the ionomer membranes as a function of relative humidity at 80 °C.

Fuel Cell Performance of the Double-Layer Ionomer Membrane. An MEA was prepared from the double-layer membrane and subjected to fuel cell performance tests. The thin Nafion layer was placed onto the cathode side. For comparison, MEAs with Nafion NRE 211 and SPK-*bl*-1 membranes were also investigated. Note that the amounts of platinum and Nafion binder were the same for all MEAs. Figure 3 shows cyclic voltammograms (CVs) of the cathode for the three cells (NRE211-cell, SPK-cell, and SPK–Nafion-cell) at 80 °C. The three cells showed similar CVs typical for polycrystalline platinum at all humidities. The electrochemically active surface areas (ECSAs) were estimated from the hydrogen adsorption charge and are plotted as a function of RH in Figure 4. ECSA values were comparable among the three cells, indicating that the contact between Pt catalysts and ionomers was similar in these catalyst layers. The CVs of the NRE211-cell were shifted upward compared to the other two cells due to the oxidation current of the cross over hydrogen. This result is reasonable, taking into account the much higher gas permeability of Nafion than that of the SPK-*bl*-1 membrane.[8] The SPK–Nafion cell exhibited a low hydrogen crossover current, as low as that of the SPK-cell, indicating the very low hydrogen permeability of the double-layer membrane. The differences in hydrogen permeability among the three membranes were further confirmed by LSVs (Figure S1, Supporting Information). The oxidation current densities at 0.4 V of the cross over hydrogen were ca. 0.1–0.3 mA cm^{-2} for the SPK– and SPK–Nafion-cells, which were much lower (<20%) than that of the NRE211-cell (ca. 1.2–1.6 mA cm^{-2}).

The fuel cell performances were investigated for the SPK–Nafion-cell and compared with those of the NRE211- and SPK-cells under the same operating conditions. Figure S2, Supporting Information, shows polarization curves (ohmic (*IR*) drop included) and ohmic resistances of the three cells. The three cells showed similar ohmic resistances and their current density dependence at humidities greater than 53% RH, which were in good accordance with the proton conductivities of the three membranes. The SPK- and SPK–Nafion-cells showed higher ohmic resistances than that of the NRE211-cell at 30% RH because of the slightly lower proton conductivity of the former membranes. At 30% RH, the ohmic resistance of the SPK-cell decreased rapidly at low current density but increased gradually when further increasing the current density, due to dehydration of the membrane. This result indicates that the SPK-*bl*-1 membrane is more likely to dehydrate than the Nafion membrane in the operating fuel cell (note that the fuel cells were operated at constant gas utilization, and gas flow rates increased with increasing current density, often causing dehydration of the membranes). Such dehydration was not observed for the SPK–Nafion-cell, which showed nearly constant ohmic resistance at current densities above 0.1 A cm^{-2}. The thin Nafion interlayer was effective in preventing the membranes from drying excessively under low-humidity conditions.

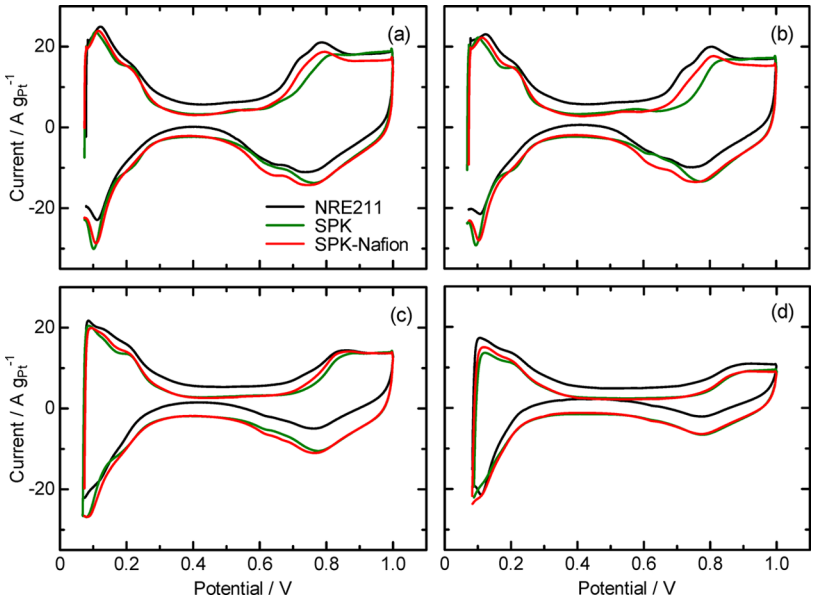

Figure 3. Cyclic voltammograms (CVs) of the NRE211-cell, SPK-cell, and SPK–Nafion-cell at 80 °C under humidity conditions of (a) 100%, (b) 80%, (c) 53%, and (d) 30% RH.

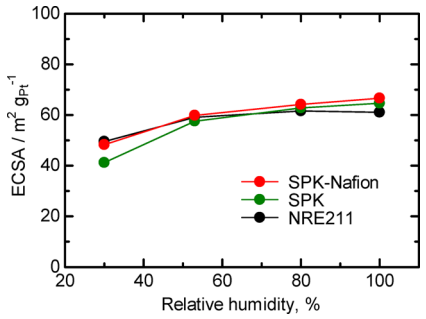

Figure 4. Humidity dependence of ECSA for the NRE211-cell, SPK-cell, and SPK–Nafion-cell at 80 °C.

The SPK-cell showed lower *I*–*V* performance than that of the NRE211-cell, although the ohmic resistances were comparable at humidities greater than 53% RH. The differences in the performance between the two cells became larger with decreasing humidity. The higher ohmic resistance of the SPK-cell than that of the NRE211-cell at 30% RH caused even larger performance differences. In order to investigate this issue in more detail, the *IR*-free polarization curves are shown in Figure 5. The SPK–Nafion-cell exhibited improved performance compared to that of the SPK-cell, and the effect of the double-layer membrane was most pronounced at 30% RH, at which humidity the performance of the SPK–Nafion-cell was nearly comparable to that of the NRE211-cell. The mass activities at 0.85 V, which are regarded as a measure of the

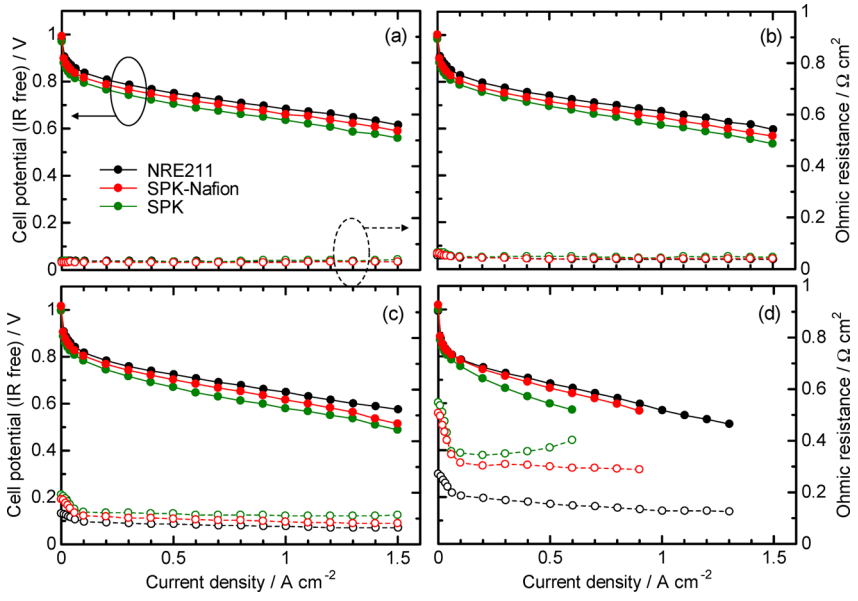

Figure 5. *IR*-corrected polarization curves and ohmic resistances of NRE211-cell, SPK-cell, and SPK–Nafion-cell at 80 °C under humidity conditions of (a) 100%, (b) 80%, (c) 53%, and (d) 30% RH.

effectiveness of Pt catalysts,[12] were calculated from the data in Figure 5 and are plotted as a function of RH in Figure 6. The

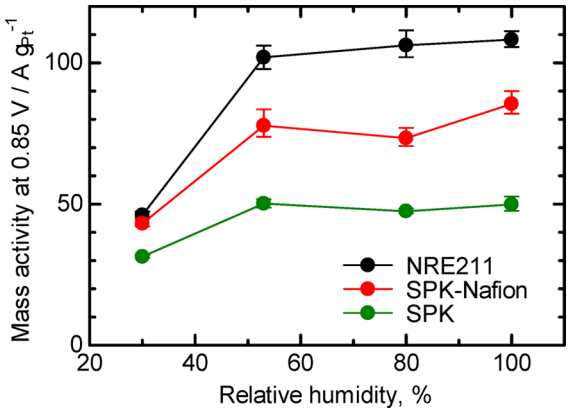

Figure 6. Mass activity at 0.85 V of NRE211-cell, SPK-cell, and SPK–Nafion-cell as a function of RH at 80 °C.

mass activity of the NRE211-cell was 108 A g_{Pt}^{-1} at 100% RH and a factor of ca. two higher than that of the SPK-cell. It is assumed that the proton transport network at the interface of the membrane and the catalyst layer is responsible. Since the SPK-*bl*-1 membrane has a large phase-separated morphology (several tens of nanometers), as previously confirmed by TEM and SAXS analyses,[13] a portion of the catalyst nanoparticles with Nafion binder might not have contacted well with the proton-conductive hydrophilic domains but attached to non-proton conductive hydrophobic domains. Such catalyst particles are covered by Nafion binder and would thus be active in the CV measurements (under nearly static conditions) to account for reasonable ECSA values but would not function in the operating fuel cells (under dynamic conditions) because of insufficient proton supply from the membrane.[12,14] The Nafion interlayer was effective in improving the interfacial contact between the SPK-*bl*-1 membrane and the cathode catalyst layer. The effect of the interlayer was most striking at 30% RH, presumably because the proton-conductive path at the surface of the SPK-*bl*-1 membrane was least developed at low humidity as confirmed by electrochemical AFM analyses.[15] The mass activity of the SPK–Nafion-cell was 43.1 A g_{Pt}^{-1} at 30% RH, which was comparable to that of the NRE211-cell (46.1 A g_{Pt}^{-1}).

CONCLUSIONS

We successfully prepared a double-layer ionomer membrane, SPK–Nafion, for improving fuel cell performance. The double-layer membrane was composed of a thin (ca. 0.55 μm), flat Nafion layer on the thick (24 μm) SPK-*bl*-1 membrane, whose phase-separated morphologies were very similar to those of the original components. The double-layer membrane exhibited comparable water uptake and proton conductivity and better fuel cell performance to those of the SPK-*bl*-1 membrane. Because of its tendency to dehydrate and its large phase-separated morphology, the SPK-*bl*-1 membrane exhibited larger ohmic resistance and lower fuel cell performance compared to those of the Nafion membrane. In the SPK–Nafion-cell, the Nafion interlayer contributed to improving the interfacial contact between the SPK-*bl*-1 membrane and the cathode catalyst layer, preventing the membrane from drying excessively. The effect of the interlayer was remarkable, since it lowered the ohmic resistance of the SPK-*bl*-1 membrane and improved the cathode catalytic performance. The mass activity at 0.85 V of the SPK–Nafion-cell was much higher than that of the SPK-cell, comparable to that of the NRE211-cell at 30% RH. The very thin Nafion interlayer successfully compensated for the shortcomings of an aromatic ionomer membrane that is promising as an alternative to PFSAs in terms of low gas crossover, high mechanical strength, good environmental compatibility, and low production cost. The results emphasize the importance of suitable design of the interfacial structures between the ionomer membrane and the catalyst layer for high-performance PEFCs, especially when applying novel proton-conducting materials as proton exchange membranes.

ASSOCIATED CONTENT

Supporting Information

LSV current density at 0.4 V and *IR*-included polarization curves. This material is available free of charge via the Internet at http://pubs.acs.org.

AUTHOR INFORMATION

Corresponding Authors

*Phone: +81 552208620. Fax: +81 552540371. E-mail: m-watanabe@yamanashi.ac.jp.

*Phone: +81 552208707. Fax: +81 552208707. E-mail: miyatake@yamanashi.ac.jp.

Notes

The authors declare no competing financial interest.

ACKNOWLEDGMENTS

This work was partly supported by the New Energy and Industrial Technology Development Organization (NEDO) through the HiPer-FC Project and the Ministry of Education, Culture, Sports, Science and Technology (MEXT) Japan through a Grant-in-Aid for Scientific Research (26289254).

REFERENCES

(1) Hickner, M. A.; Ghassemi, H.; Kim, Y. S.; Einsla, B. R.; McGrath, J. E. Alternative Polymer System for Proton Exchange Membrane (PEMs). *Chem. Rev.* **2004**, *104*, 4587–4612.

(2) Dupuis, A.-C. Proton Exchange Membranes for Fuel Cells Operated at Medium Temperatures: Materials and Experimental Techniques. *Prog. Mater. Sci.* **2011**, *56*, 289–327.

(3) Sethuraman, V. A.; Weidner, J. W.; Haug, A. T.; Protsailo, L. V. Durability of Perfluorosulfonic Acid and Hydrocarbon Membranes: Effect of Humidity and Temperature. *J. Electrochem. Soc.* **2008**, *155*, B119–B124.

(4) Dhara, M. G.; Banerjee, S. Fluorinated High-Performance Polymers: Poly(arylene ether)s and Aromatic Polyimides Containing Trifluoromethyl Groups. *Prog. Polym. Sci.* **2010**, *35*, 1022–1077.

(5) Park, C. H.; Lee, C. H.; Guiver, M. D.; Lee, Y. M. Sulfonated Hydrocarbon Membranes for Medium-Temperature and Low-Humidity Proton Exchange Membrane Fuel Cells (PEMFCs). *Prog. Polym. Sci.* **2011**, *36*, 1443–1498.

(6) Li, N.; Guiver, M. D. Ion Transport by Nanochannels in Ion-Containing Aromatic Copolymers. *Macromolecules* **2014**, *47*, 2175–2198.

(7) Okanishi, T.; Yoda, T.; Sakiyama, Y.; Miyahara, T.; Miyatake, K.; Uchida, M.; Watanabe, M. Durability of an Aromatic Block Copolymer Membrane in Practical PEFC Operation. *Electrochem. Commun.* **2012**, *24*, 47–49.

(8) Miyahara, T.; Hayano, T.; Matsuno, S.; Watanabe, M.; Miyatake, K. Sulfonated Polybenzophenone/Poly(arylene ether) Block Copolymer Membranes for Fuel Cell Applications. *ACS Appl. Mater. Interfaces* **2012**, *4*, 2881–2884.

(9) Jung, M. S.; Kim, Y. J.; Yoon, Y. J.; Kang, C. G.; Yu, D. M.; Lee, J. Y.; Kim, H.-J.; Hong, Y. T. Sulfonated Poly(arylene sulfone) Multiblock Copolymers for Proton Exchange Membrane Fuel Cells. *J. Membr. Sci.* **2014**, *459*, 72−85.
(10) Kim, Y. S.; Pivovar, B. S. The Membrane-Electrode Interface in PEFCs IV. The Origin and Implications of Interfacial Resistance. *J. Electrochem. Soc.* **2010**, *157*, B1616−B1623.
(11) Carter, R. N.; Brady, B. K.; Subramanian, K.; Tighe, T.; Gasteiger, H. A. Spatially Resolved Electrode Diagnostic Technique for Fuel Cell Applications. *J. Electrochem. Soc.* **2007**, *11*, 423−433.
(12) Lee, M.; Uchida, M.; Yano, H.; Tryk, D. A.; Uchida, H.; Watanabe, M. New Evaluation Method for the Effectiveness of Platinum/Carbon Electrocatalysts under Operating Conditions. *Electrochim. Acta* **2010**, *55*, 8504−8512.
(13) Mochizuki, T.; Kakinuma, K.; Uchida, M.; Deki, S.; Watanabe, M.; Miyatake, K. Temperature- and Humidity-Controlled SAXS Analysis of Proton-Conductive Ionomer Membranes for Fuel Cells. *ChemSusChem* **2014**, *7*, 729−733.
(14) Watanabe, M.; Sakairi, K.; Inoue, M. An effect of Proton Conductivity in Electrolyte Membranes on Cathode Performances at Polymer Electrolyte Fuel Cells. *J. Electroanal. Chem.* **1994**, *375*, 415−418.
(15) Hara, M.; Miyahara, T.; Hoshi, T.; Ma, J.; Hara, M.; Miyatake, K.; Inukai, J.; Alonso-Vante, N.; Watanabe, M. Proton Conductive Areas on Sulfonated Poly(arylene ketone) Multiblock Copolymer Electrolyte Membrane Studied by Current-Sensing Atomic Force Microscopy. *Electrochemistry* **2014**, *82*, 369−375.